



Cite this: DOI: 10.1039/c5ra24656c

Explaining stability of transition metal carbides – and why TcC does not exist†

 Qinggao Wang,^{*ae} Konstantin E. German,^{bg} Artem R. Oganov,^{acdf} Huafeng Dong,^d Oleg D. Feys,^a Ya. V. Zubavichus^h and V. Yu. Murzin^h

We analyze the formation of transition metal (TM) carbides, as determined by the strength of TM–TM and TM–C bonds, as well as lattice distortions induced by C interstitials. With increasing filling of the d-band of TMs, TM–C bonds become increasingly weak from the left of the periodic table to the right, with fewer and fewer C atoms entering the TMs lattice. Technetium (Tc) turns out to be a critical point for the formation of carbides, guiding us to resolve a long-standing dispute. The predicted Tc carbides, agreeing with measured X-ray absorption spectra, should decompose to cubic Tc and graphite above 2000 K. Consequently, we show that what has been claimed as TcC (with rocksalt structure) is actually a high-temperature cubic phase of elemental technetium.

 Received 20th November 2015
 Accepted 29th January 2016

DOI: 10.1039/c5ra24656c

www.rsc.org/advances

Transition metal carbides (TM_xC_y , $x \geq y$) have attracted increasing attention due to their “platinum-like” electronic structures, high hardnesses and melting temperatures, and good thermal and electrical conductivities.^{1–6} Due to these properties, TM_xC_y compounds are not only advanced materials that can be applied in extreme environments, but also a most promising kind of low-cost catalyst. Mo carbides are used as catalysts for hydrogen production reactions,^{7,8} but the activities of $\gamma\text{-MoC}$ and $\beta\text{-Mo}_2\text{C}$ are different.⁹ Detailed knowledge of TM_xC_y compounds is the key for related material designs, but the field is marked by many controversies. For example, Wang *et al.* suggested the synthesis of CrC ,¹⁰ but some other researchers thought it was impossible.¹¹ To guide studies in the future, it is important to know which TM_xC_y compounds are possible, and why.

Groups IVB and VB TM_xC_y compounds usually are monocarbides with NaCl structure (TiC , ZrC , HfC , VC , NbC and TaC), while compounds of group VIB TM_xC_y have different structures

and stoichiometries, *e.g.* Mo_2C , W_2C and WC (ref. 2). Further increasing the filling of d-band (*i.e.*, for TMs at the right side of the periodic table), only TM-rich carbides were obtained, *e.g.*, Fe_3C .¹² Consistent with nonstoichiometry, TM_2C , TM_4C_3 , TM_3C_2 , TM_6C_5 , and TM_8C_7 superstructures may form, and their structures were predicted recently.^{13,14} Indeed, Ta_6C_5 , Ta_2C , Ta_4C_3 , Ta_3C_2 , Hf_3C_2 , and Hf_6C_5 were found to be thermodynamically stable for Ta–C¹⁵ and Hf–C⁶ systems, respectively, with the help of the evolutionary algorithm USPEX.^{16,17} Although it is possible to make detailed and reliable numerical predictions, a general understanding of the formation of TM_xC_y compounds is still lacking.

The trend of stability for transition metal carbides

We can consider C atoms in TM_xC_y compounds as interstitials in the TM-sublattice. As a result of inserting carbon atoms, TM–TM bonds are weakened, but this is compensated by the formation of TM–C bonds. Stability of carbides depends on the detailed balance between these factors. As reported,¹⁸ nobleness increases from left to right for 3d, 4d and 5d TMs. Corresponding TM–C bonds should become weaker and weaker, and thus fewer and fewer C atoms could enter the TMs lattice. Therefore, C content in TM_xC_y compounds, per TM atom, should decrease from left to right for TMs in the periodic table.

The strength of TM–TM bonds is revealed by the cohesive energy of a TM (E_{Coh}), which is computed as

$$E_{\text{Coh}} = -\left(\frac{1}{n}E_{\text{TM}}^{\text{bulk}} - E_{\text{TM}}^{\text{atom}}\right), \quad (1)$$

^aMoscow Institute of Physics and Technology, 9 Institutskiy Lane, Dolgoprudny City, Moscow Region, 141700, Russia. E-mail: wangqinggao1984@126.com

^bA.N. Frumkin Institute of Physical Chemistry and Electrochemistry RAS, Leninsky pr. 31, 119991 Moscow, Russia

^cSkolkovo Institute of Science and Technology, Skolkovo Innovation Center, 3 Nobel St., Moscow 143026, Russia

^dDepartment of Geosciences and Center for Materials by Design, Stony Brook University, Stony Brook, New York 11794, USA

^eDepartment of Physics and Electrical Engineering, Anyang Normal University, Anyang, Henan Province, 455000, People's Republic of China

^fInternational Center for Materials Discovery, Northwestern Polytechnical University, Xi'an, Shanxi 710072, People's Republic of China

^gMedical University Reaviz, Krasnobogatyrskaya 2, Moscow 107564, Russia

^hRussian Research Center Kurchatov Institute, Moscow 123182, Russia

† Electronic supplementary information (ESI) available. See DOI: 10.1039/c5ra24656c

where $\frac{1}{n}E_{\text{TM}}^{\text{bulk}}$ is the total energy of a TM normalized per atom, and $E_{\text{TM}}^{\text{atom}}$ is the total energy of an isolated TM atom. As seen in Fig. 1, E_{Coh} values do not vary monotonically change, especially for 3d TMs.

At low C contents, the strength of TM–C bonds is estimated using the energy of formation of a dilute C interstitial in a TM, for example, with resulting stoichiometry TM_{16}C . The C dissolution energy ($E_{\text{C-dis}}$) is defined as

$$E_{\text{C-dis}} = E_{\text{TM}_{16}\text{C}} - E_{\text{TM}_{16}}^{\text{bulk}} - \frac{1}{m}E(\text{graphite}), \quad (2)$$

where $E_{\text{TM}_{16}}^{\text{bulk}}$ and $E_{\text{TM}_{16}\text{C}}$ are total energies of TM and TM_{16}C , respectively. $\frac{1}{m}E(\text{graphite})$ is the total energy of graphite normalized per atom. Negative (positive) $E_{\text{C-dis}}$ values mean that C atoms would (would not) like to occupy octahedral sites. Except for group VIB TMs, $E_{\text{C-dis}}$ values decrease from left to right (Fig. 1).

In MoC and WC, carbon atoms occupy trigonal prismatic sites,⁵ corresponding to positive $E_{\text{C-dis}}$ values. In contrast, C atoms in TiC, ZrC, HfC, VC, NbC and TaC occupy octahedral sites² and have negative $E_{\text{C-dis}}$ values. At a high C content, the strength of TM–C bonds is estimated by NaCl- or WC-type TM monocarbide, which could be chosen according to $E_{\text{C-dis}}$ values. The formation energy of a TM monocarbide is defined as

$$E_{\text{TMC}} = E_{\text{TMC}}^{\text{bulk}} - \frac{1}{n}E_{\text{TM}}^{\text{bulk}} - \frac{1}{m}E(\text{graphite}), \quad (3)$$

where $E_{\text{TMC}}^{\text{bulk}}$ is the total energy of a certain TM monocarbide. Negative E_{TMC} values indicate that monocarbides are thermodynamically stable.

Charge transfer contributes to the strength of TM–C bonds in TM_xC_y compounds, and is defined as:

$$\Delta C_{\text{chg}} = C_{\text{chg}}(\text{TMC}) - C_{\text{chg}}(\text{graphite}), \quad (4)$$

where $C_{\text{chg}}(\text{TMC})$ and $C_{\text{chg}}(\text{graphite})$ are Bader charges of a C atom in a TM monocarbide and in graphite, respectively. Bader analysis was performed using grid-based algorithm.¹⁹ In Fig. 1, ΔC_{chg} values are larger for TMs at the left side of the periodic table, indicating that there TM–C bonds are stronger. In agreement with this tendency, a theoretical calculation indicates that the formation of a C vacancy in ZrC costs 58 mRy at 0 K, and it is more difficult than that in NbC (42 mRy).²⁰

Negative $E_{\text{C-dis}}$ values correlate with E_{TMC} for NaCl-type monocarbides, since their local structure is similar. E_{TMC} values are -1.62 , -1.63 , -1.88 , -0.83 , -1.06 and -1.17 eV for TiC, ZrC, HfC, VC, NbC and TaC, respectively, showing a strong thermodynamic driving force for their formation. For elements forming WC-type monocarbides, $E_{\text{C-dis}}$ values turn out to be positive: 1.65 and 1.99 eV for Mo_{16}C and W_{16}C , respectively, and E_{TMC} values are -0.18 and -0.24 eV for MoC and WC, respectively, again consistent with their observed formation.

The COOP (Crystal Orbital Overlap Population) analysis reveals that the covalency of Fe- and Mn–C bonds is not as strong as that of Mo–C and W–C bonds.²¹ FeC and MnC are unstable according to their positive E_{TMC} values, and one could conclude that strong covalency of TM–C bonds is essential for the formation of WC-type monocarbides. At reduced C contents, Fe- and Mn-rich carbides become stable (highlighted by the green box) due to the reduced distortion of TMs lattice. Through the same mechanism, TM-rich carbides of group IVB TMs are also stable at lower C contents, e.g., Hf_3C_2 and Hf_6C_5 ,⁶ although stoichiometric HfC is also stable.

E_{TMC} values of WC-type RuC and OsC are 0.51 and 1.84 eV, respectively, implying their instability. Ru and Os are more inert (noble), since their d-band fillings are larger.¹⁸ Positive $E_{\text{C-dis}}$ values for Ru_{16}C (1.70 eV) and Os_{16}C (2.85 eV) further manifest the nobleness of Ru and Os, i.e., no carbides form even at low concentrations of carbon. Hypothetical, but now clearly impossible, OsC and RuC were considered as superhard materials.^{4,22} In the same group of the periodic table, Fe-rich carbides (e.g., Fe_3C^{12}) are stable because the E_{Coh} value (5.03 eV) of Fe is smaller than those of Ru (7.86 eV) and Os (8.50 eV). Therefore, the formation of carbides is more favorable for TMs with smaller E_{Coh} values.

According to TMs nobleness,¹⁸ Re–C bonds are stronger than Ru–C and Os–C bonds. Therefore, Re carbides would be more likely to form, yet this factor alone is not sufficient, and our USPEX calculation does not find any stable Re carbide (see ESI†). To sum up, there are no stable carbides for Re, Ru and Os. In contrast, C atoms could enter Tc lattice according to the $E_{\text{C-dis}}$ value of Tc_{16}C (-0.02 eV), but the formation of TcC is impossible because of its positive E_{TMC} (0.27 eV). Consequently, only Tc-rich carbides may be stable.

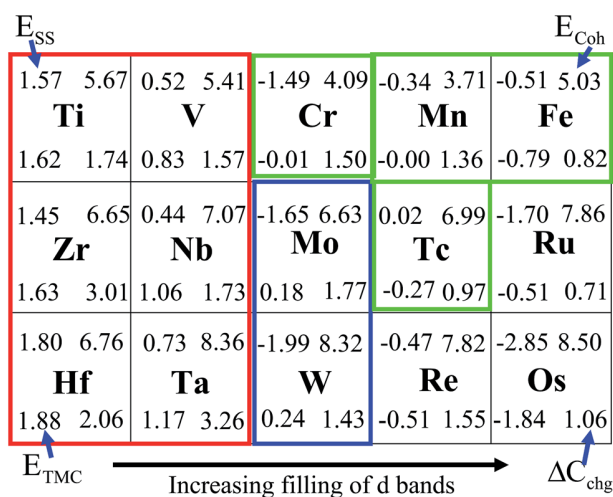


Fig. 1 Cohesive energies of TMs (E_{Coh}), C dissolution energies calculated using TM_{16}C model ($E_{\text{C-dis}}$), formation energies of TM monocarbides (E_{TMC}), and charges captured by C atoms in TM monocarbides (ΔC_{chg}). NaCl- or WC-type TM monocarbides are selected in the light of $E_{\text{C-dis}}$ values.

The controversy on technetium carbide

As a spent-fuel waste of ^{235}U fission, radiotoxic ^{99}Tc is dangerous due to its growing inventory and environmental

mobility.²³ This challenge can be treated by Tc transmutation ($^{99}\text{Tc} \rightarrow ^{100}\text{Tc} \rightarrow ^{100}\text{Ru} \rightarrow ^{101}\text{Ru}$),²⁴ but the extraction of pure Tc is quite difficult. Tc carbides are promising alternative target materials (ref. 25), whose lattice expansion may alleviate resonance shielding of thermal neutrons in transmutation.²⁴ About fifty years ago, it was proposed that TcC is the observed high-temperature cubic phase,^{26,27} and it was accepted both experimentally²⁸ and theoretically.²⁹ Yet, that phase was also interpreted as cubic Tc on the basis of nuclear magnetic resonance (NMR) data.^{30,31} Furthermore, a cubic phase is present in samples covering a wide range of C content.²⁵ To summarize, it is unclear what the observed high-temperature cubic phase is, and this long-standing puzzle is of great scientific and technological significance.

Theoretical calculations

To resolve the controversy on technetium carbide and check our qualitative trend of stability of TM carbides, we searched for all stable Tc carbides using the USPEX code.^{16,17} Eighty structures (with any compositions between pure Tc and pure C, with up to 20 atoms in the primitive unit cell) were randomly produced in the first generation. Each of the subsequent 59 generations contained 50 structures, of which 30%, 30%, 20%, and 20% were produced by heredity, symmetric random algorithm, softmutation and transmutation operators, respectively. Relaxations of candidate structures were done by the VASP code,^{32,33} for exchange–correlation using the generalized gradient approximation in the Perdew–Burke–Ernzerhof form.³⁴ Core electrons were treated using the projector-augmented wave method,³⁵ with the plane-wave kinetic energy cutoff of 700 eV. We used uniform I -centered k -points meshes with reciprocal-space resolution of $2\pi \times 0.05 \text{ \AA}^{-1}$. These settings produced well-converged results. Stability of compounds was determined using the thermodynamic convex hull construction, where compounds/structures on the convex hull are stable, and those above the convex hull are metastable. The effects of temperature on the stability of compounds were investigated within the quasiharmonic approximation, using the Phonopy code.³⁶

Consistent with the trend of stability of TM carbides, three possible Tc-rich carbides are predicted, which are Tc_{10}C , Tc_8C and Tc_6C . Their crystal structures are given in ESI.† At 0 K, only Tc_8C is stable. Actually, Tc-rich carbides with different carbon concentrations have been experimentally obtained.²⁵ To rationalize the experimental result, we define the formation energy of Tc-rich carbides normalized per Tc atom,

$$E_{\text{Tc}_x\text{C}} = 1/x \left(E_{\text{Tc}_x\text{C}} - xE_{\text{Tc}} - \frac{1}{m} E(\text{graphite}) \right), \quad (5)$$

where E_{Tc} and $E_{\text{Tc}_x\text{C}}$ are the total energies (per atom) of bulk Tc and Tc_xC carbide, respectively. $E_{\text{Tc}_x\text{C}}$ values increase with C concentrations, *i.e.*, $E_{\text{Tc}_{10}\text{C}} (-0.005 \text{ eV}) < E_{\text{Tc}_8\text{C}} (-0.015) < E_{\text{Tc}_6\text{C}} (-0.017 \text{ eV})$. Driven by the thermodynamics, the formation of Tc carbides depends on C content, and maximally 16.7 at% C could enter Tc lattice. These results are in agreement with experimental results, excess carbon was present in samples when total C content exceeded 17 at%.²⁵ Thus, the experimental finding,

where Tc carbides have different C concentrations,²⁵ is rationalized theoretically.

The formation of Tc carbides can be viewed as a process of inserting carbon atoms into Tc lattice, resulting in a lattice expansion. Compared with hcp Tc (14.59 \AA^3), the increments of specific cell volume (normalized per Tc atom) are 4.66%, 5.55% and 7.74% for Tc_{10}C (15.27 \AA^3), Tc_8C (15.40 \AA^3) and Tc_6C (15.72 \AA^3), respectively. The first two specific cell volumes (15.55 and 15.65 \AA^3) measured in the experiment²⁵ are larger than that of Tc_8C . However, the third measurement (15.75 \AA^3) is in excellent agreement with the specific cell volume of Tc_6C , and it does not further increase with C content (above 17 at%).²⁵ These results reveal that the formation of Tc carbides depends on C content, and the maximum C concentration is about 17 at%, corresponding to Tc_6C .

Experimental investigations

In the light of theoretical prediction, Tc_6C , having the maximum C concentration, can be easily confirmed experimentally. The synthesis of Tc_xC microcrystallites was carried out according to the procedure of a previous paper.²⁵ The sample with 50 at% C was less fused and could be destroyed easily, revealing the mixture of carbides and graphite. For X-ray absorption measurements, we powered the sample and homogenized it with BN (10 mg Tc_xC + C-50 mg BN), and then pressed into a special plastic holder of an ESRF-ROBLE device.

The extended X-ray absorption fine structure (EXAFS) and X-ray absorption near-edge spectra (XANES) of Tc K-edge were measured at the Structural Materials Science Station (Russian Research Centre Kurchatov Institute)³⁷ in a transmission geometry, using a Si(111) monoblock monochromator with a slit and two ionization chambers filled with argon–xenon mixture gas. The EXAFS spectra were extracted using Athena and Artemis programs in IFEFFIT package.³⁸ The multisphere fitting of normalized EXAFS curves $\chi(k)$ was performed in a photoelectron wavenumber range k 3.0–16.0 \AA^{-1} , with the k^3 weight scheme using the photoelectron phases and scattering amplitudes, calculated by FEFF program.³⁹

The amplitudes of Fourier transform of XANES spectra are shown in Fig. 2 for the Tc_xC sample with 50 at% C. The XANES data indicate that a Tc atom is surrounded by 12 Tc atoms at a distance of 2.72 \AA , corresponding to a close-packed structure.

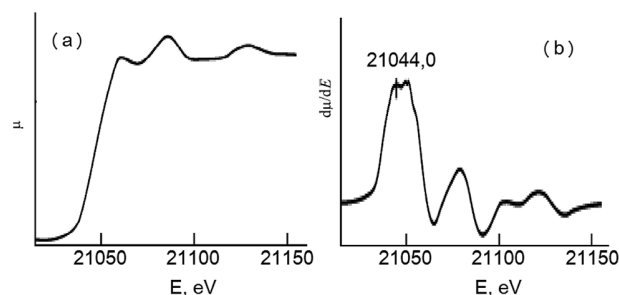


Fig. 2 XANES spectrum of (a) Tc K-edge, and (b) the first derivative for the Tc_xC sample with 50 at% C.

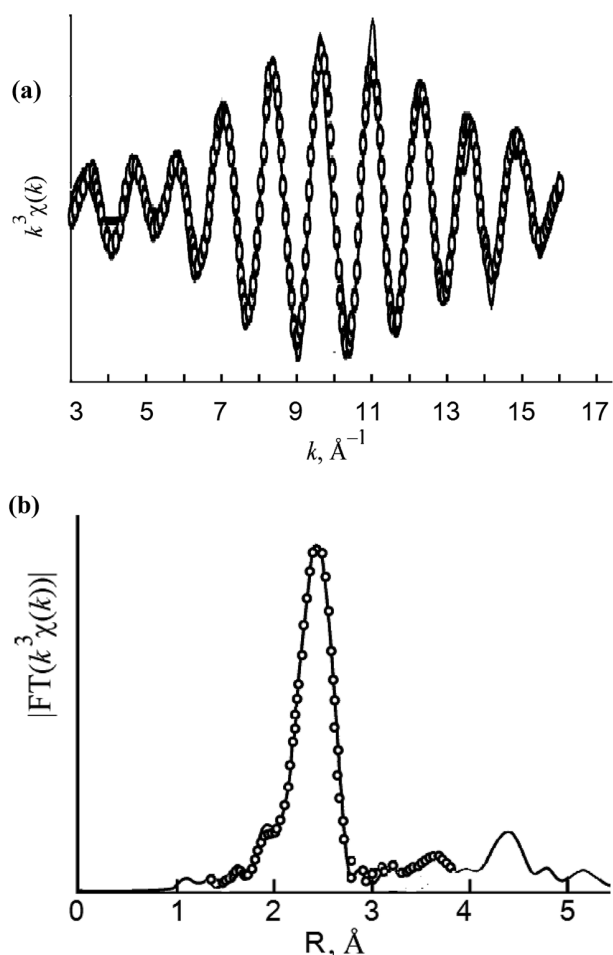


Fig. 3 (a) Experimental curve of normalized EXAFS signal (solid line) and optimized theoretical curve (points), and (b) modulus of the Fourier transform for the experimental EXAFS spectrum (solid) and its optimized theoretical curve (circle points) for the Tc_xC sample with 50 at% C (parameters of local structure are given in Table 1).

Table 1 Parameters of the local structure for the Tc_xC sample with 50 at% C according to EXAFS data: coordination numbers N , interatomic distances R , and Debye–Waller parameters σ^2 ($k = 3.0\text{--}16.6$, $R = 1.8\text{--}3.0$ Å, $\Delta E = 17.0$ eV, $R_f = 0.004$)

Sample	Scattering path	N	R , Å	σ^2 , Å ²
Tc_xC	Tc–Tc	12	2.72	0.0057

The normalized EXAFS curves are shown in Fig. 3. The spectrum of Tc_xC sample with 50 at% C is very similar to the reference spectrum of Tc_3C obtained in.⁴⁰ These results indicate the identity of carbides in the samples having 17 at% and 50 at% C. Combined with predicted Tc carbides and their increments of specific cell volumes, we unhesitatingly conclude that the solubility of carbon in Tc cannot exceed 17 at%. In brief, the predicted Tc_6C has the largest C concentration.

High-temperature cubic phase of elemental technetium

In the past, a high-temperature cubic phase was taken for NaCl-type TcC ,^{26,27} but this cubic phase was also proposed to be pure technetium in the light of NMR results.^{30,31} This long-standing puzzle, of great scientific and technological significance, could be solved with the help of the trend of stability of TM carbides. Namely, NaCl-type TcC cannot be the high-temperature cubic phase observed in experiments. The lattice of cubic Tc is different from the Tc sublattice of NaCl-type TcC (Fig. 4), due to significant lattice expansion caused by C interstitials in TcC . And thus, their XRD spectra should be different. To prove this conclusion, we simulated the XRD spectra of cubic Tc and NaCl-type TcC . The main peak of cubic Tc is located at $2\theta = 40^\circ$ (with X-ray wavelength 1.540562 Å), which is the same as the experimental result (Fig. 4a).²⁵ However, the XRD spectrum of TcC deviates from the experimental observation, having the main peak at $2\theta = 36^\circ$. Once again, we demonstrate that Tc rather than TcC , accords with the high-temperature cubic phase obtained in experiments.^{25–27}

Of course, our calculation predicts that at high temperature the cubic structure will be elemental technetium. This can be directly checked, and we performed quasiharmonic free energy calculations to investigate relative stability of the fcc and room-temperature hexagonal (hcp) forms of technetium. Above 1775 K, cubic (fcc) Tc is more stable than the hcp phase of Tc (Fig. 5), due to its larger vibration entropy. This result roughly agrees with an experimental conclusion that the cubic phase is stable above 1835 °C (2108 K),²⁶ in which the deviation of transition temperature may be caused by disordered interstitial carbon atoms. Their concentration (x) can be roughly estimated through considering the E_{C-dis} of fcc-Tc and contribution of configurational entropy, *i.e.*, $RT[x \ln x + (1-x)\ln(1-x)]$. Even at 2000 K, the maximum concentration of disordered carbon is in

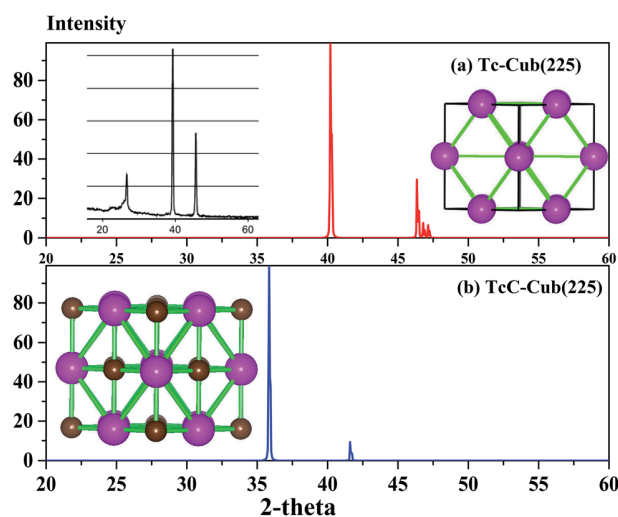


Fig. 4 In the inset in (a), we show the experimental XRD pattern of Tc metal and (b) NaCl-type TcC with the X-ray wavelength of 1.540562 Å. In (a), we illustrate the experimental XRD of Tc metal annealed with 50 at% C.²⁵

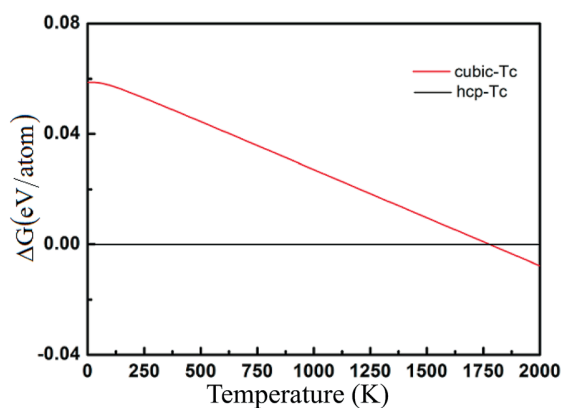


Fig. 5 Stability of hexagonal and cubic Tc as a function of temperature.

the region of $7.67 \text{ at}\% < x < 11.1 \text{ at}\%$. To sum up, Tc rather than TcC, is the observed high-temperature cubic phase.^{26,27}

Discussions

Trends of stability for TM carbides can be easily rationalized, as we have shown above. With increasing filling of the d-band, TM–C bonds become weaker and weaker from left to right of the periodic table for 3d, 4d and 5d TM series. This diminishes the thermodynamic driving force for incorporation of C atoms in the TMs lattice; Tc corresponds to the break point, with easy carbide formation to its left and no carbide formation to its right. This rule easily explains why such compounds as TcC^{29,41} and OsC⁴ are impossible. Formation of multiphase assemblages often obscures experimental analysis, but theoretical calculations can bring clarity and explain which phases could have been synthesized and what their properties are likely to be. For example, a multiphase of Mo carbides was synthesized, as low-cost catalysts for hydrogen evolution reactions.⁹ As reported,¹³ many TM_xC_y compounds may remain unidentified, but recent theoretical discoveries of such compounds^{6,14,15} suggest that state-of-art theoretical approaches will play an increasingly important role in further discovery of TM_xC_y compounds, and such discoveries can be greatly aided by simple trends, such as the one discussed here.

Acknowledgements

This research is supported by the Government of the Russian Federation (No. 14.A12.31.0003). Qinggao Wang acknowledges the National Natural Science Foundation of China (Grant No. 11504004) and the “5top100” postdoctoral fellowship conducted at Moscow Institute of Physics and Technology (MIPT). Calculations were performed on the Rurik supercomputer of our laboratory at Moscow Institute of Physics and Technology.

References

- 1 L. H. Bennett, J. R. Cuthill, A. J. McAlister, N. E. Erickson and R. E. Watson, *Science*, 1974, **184**, 563–565.
- 2 H. H. Hwu and J. G. Chen, *Chem. Rev.*, 2005, **105**, 185–212.
- 3 W.-F. Chen, J. T. Muckerman and E. K. Fujita, *Chem. Commun.*, 2013, **49**, 8896.
- 4 J.-C. Zheng, *Phys. Rev. B: Condens. Matter Mater. Phys.*, 2005, **72**, 052105.
- 5 H. W. Hugosson, U. Jansson, B. Johansson and O. Eriksson, *Science*, 2001, **293**, 2434–2437.
- 6 Q. Zeng, J. Peng, A. R. Oganov, Q. Zhu, C. Xie, X. Zhang, D. Dong, L. Zhang and L. Cheng, *Phys. Rev. B: Condens. Matter Mater. Phys.*, 2013, **88**, 214107.
- 7 M. Wu, X. Lin, A. Hagfeldt and T. Ma, *Angew. Chem., Int. Ed.*, 2011, **50**, 3520–3524.
- 8 P. Xiao, X. Ge, H. Wang, Z. Liu, A. Fisher and X. Wang, *Adv. Funct. Mater.*, 2015, **25**, 1520–1526.
- 9 C. Wan, Y. N. Regmi and B. M. Leonard, *Angew. Chem.*, 2014, **126**, 6525–6528.
- 10 J. Wang, X. F. Wu, B. X. Liu and Z. Z. Fang, *Acta Metall. Mater.*, 1992, **40**, 1417–1420.
- 11 F. Vines, C. Sousa, P. Liu, J. A. Rodriguez and F. Illas, *J. Chem. Phys.*, 2005, **122**, 174709.
- 12 Y. Hu, J. O. Jensen, W. Zhang, L. N. Cleemann, W. Xing, N. J. Bjerrum and Q. Li, *Angew. Chem., Int. Ed.*, 2014, **53**, 3675–3679.
- 13 A. I. Gusev, *Phys.-Usp.*, 2014, **57**, 839.
- 14 X.-X. Yu, C. R. Weinberger and G. B. Thompson, *Comput. Mater. Sci.*, 2016, **112**, 318–326.
- 15 X.-X. Yu, C. R. Weinberger and G. B. Thompson, *Acta Mater.*, 2014, **80**, 341–349.
- 16 A. R. Oganov and C. W. Glass, *J. Chem. Phys.*, 2006, **124**, 244704.
- 17 A. O. Lyakhov, A. R. Oganov, H. T. Stokes and Q. Zhu, *Comput. Phys. Commun.*, 2012, **184**, 1172–1182.
- 18 B. Hammer and J. K. Nørskov, *Nature*, 1995, **376**, 238–240.
- 19 W. Tang, E. Sanville and G. Henkelman, *J. Phys.: Condens. Matter*, 2009, **21**, 084204.
- 20 H. W. Hugosson, O. Eriksson, U. Jansson and B. Johansson, *Phys. Rev. B: Condens. Matter Mater. Phys.*, 2001, **63**, 134108.
- 21 S. D. Wijeyesekera and R. Hoffmann, *Organometallics*, 1984, **3**, 949–961.
- 22 J. C. Grossman, A. Mizel, M. Cote, M. L. Cohen and S. G. Louie, *Phys. Rev. B: Condens. Matter Mater. Phys.*, 1999, **60**, 6343–6347.
- 23 J. P. Icenhower, N. Qafoku, J. M. Zachara and W. J. Martin, *Am. J. Sci.*, 2010, **310**, 721–752.
- 24 R. J. M. Konings and R. Conrad, *J. Nucl. Mater.*, 1999, **274**, 336–340.
- 25 K. E. German, V. F. Peretrukhin, K. N. Gedgovd, M. S. Grigoriev, A. V. Tarasov, Y. V. Plekhanov, A. G. Maslennikov, G. S. Bulatov, V. P. Tarasov and M. Lecomte, *J. Nucl. Radiochem. Sci.*, 2005, **6**, 211–214.
- 26 A. L. Giorgi and E. G. Szklarz, *J. Less-Common Met.*, 1966, **11**, 455–456.
- 27 W. Trzebiatowski and J. Rudziński, *Zeitschrift für Chemie*, 1962, **2**, 158.
- 28 V. N. Eremenko, T. Y. Velikanova and A. A. Bondar, *Soviet Powder Metallurgy and Metal Ceramics*, 1989, **28**, 868–873.

- 29 Y. Liang, C. Li, W. Guo and W. Zhang, *Phys. Rev. B: Condens. Matter Mater. Phys.*, 2009, **79**, 024111.
- 30 J. Fraissard, O. Lapina, V. P. Tarasov, Y. B. Muravlev, N. N. Popova and K. E. Guerman, in *Magnetic Resonance in Colloid and Interface Science*, Springer, Netherlands, 2002, vol. 76, pp. 455–468.
- 31 V. P. Tarasov, Y. B. Muravlev, K. E. German and N. N. Popova, *Dokl. Phys. Chem.*, 2001, **377**, 71–76.
- 32 G. Kresse and J. Hafner, *Phys. Rev. B: Condens. Matter Mater. Phys.*, 1993, **47**, 558–561.
- 33 G. Kresse and J. Furthmuller, *Phys. Rev. B: Condens. Matter Mater. Phys.*, 1996, **54**, 11169–11186.
- 34 J. P. Perdew, K. Burke and M. Ernzerhof, *Phys. Rev. Lett.*, 1996, **77**, 3865–3868.
- 35 P. E. Blochl, *Phys. Rev. B: Condens. Matter Mater. Phys.*, 1994, **50**, 17953–17979.
- 36 A. Togo, F. Oba and I. Tanaka, *Phys. Rev. B: Condens. Matter Mater. Phys.*, 2008, **78**, 134106.
- 37 A. A. Chernyshov, A. A. Veligzhanin and Y. V. Zubavichus, *Nucl. Instrum. Methods Phys. Res., Sect. A*, 2009, **603**, 95–98.
- 38 B. Ravel and M. Newville, *J. Synchrotron Radiat.*, 2005, **12**, 537–541.
- 39 A. L. Ankudinov, B. Ravel, J. J. Rehr and S. D. Conradson, *Phys. Rev. B: Condens. Matter Mater. Phys.*, 1998, **58**, 7565–7576.
- 40 K. E. German, A. B. Melentev, Y. V. Zubavichyus, S. N. Kalmykov, A. A. Shiryaev and I. G. Tananaev, *Radiochemistry*, 2011, **53**, 178–185.
- 41 X.-W. Sun, Y.-D. Chu, Z.-J. Liu, T. Song, J.-H. Tian and X.-P. Wei, *Chem. Phys. Lett.*, 2014, **614**, 167–170.